

FUNCTIONALLY-GRADED NPR (NEGATIVE POISSON'S RATIO) MATERIAL FOR A BLAST-PROTECTIVE DEFLECTOR

Zheng-Dong Ma, PhD
University of Michigan
Ann Arbor, MI

Hongxin Bian, PhD
Ce Sun, PhD
MKP Structural Design
Associates, Inc.
Dexter, MI

Gregory M. Hulbert, PhD
University of Michigan
Ann Arbor, MI

Krishan Bishnoi
Farzad Rostam-Abadi
US Army TARDEC
Warren, MI

ABSTRACT

A functionally-graded NPR (Negative Poisson's Ratio) material concept has been developed for a critical Army application – blast protection. The objective is to develop a combined computational design methodology and innovative structural-material concept for a blast-protective deflector, which can concentrate material into areas most needed and adapt its shape utilizing the blast energy to improve blast mitigation and crew protection. Included in the computational design methodology is optimal deflector shape design and optimal NPR material distribution to further improve the protection while minimizing the C.G. height of the vehicle and the weight of the deflector. Structures fabricated using this new concept react to the explosion and reconfigure themselves under the blast force to provide maximum blast protection. The presented research work consists of two basic approaches to deflector design: optimal deflector shape design and optimal NPR material configuration and distribution in the innovative deflector.

INTRODUCTION

Negative Poisson's Ratio (NPR) material, also known as auxetic material [1-2], has attracted attention due to its unique behavior. Unlike conventional materials, a NPR material may shrink when compressed along a perpendicular direction, which results in a unique feature that the material can concentrate itself under the compressive load to better resist the load. It also becomes stiffer and stronger when the amplitude of the load increases. It has been found that NPR can improve material/structural properties, including enhanced thermal/shock resistance, fracture toughness, indentation resistance and shear modulus, etc. [1-3]. A range of man-made NPR materials/structures have been investigated, such as keyed brick structures, typical cellular materials (honeycombs and foams), micro-porous polymers, and molecular NPR materials, and some of them have been successfully fabricated [4-7]. A three-dimensional version of NPR materials [8] has been developed by the authors with potential usage for a variety of applications, including a blast protective structure shown in Fig. 1.

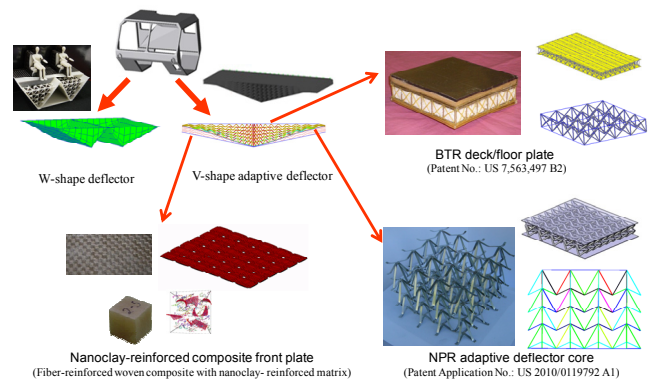


Figure 1: A lightweight, shape adaptive blast deflector concept.

Figure 1 illustrates an example three-dimensional NPR material in a lightweight, shape adaptive blast deflector concept, which is being developed under TARDEC support for significantly improved blast protection with reduced vehicle weight. The objective is to develop a new technology with associated modeling, simulation and design methodology and innovative structural-material concept for a blast-protective deflector, which can concentrate material into the areas most needed and adapt its shape utilizing the blast energy to improve blast mitigation and crew protection. This effort is also combined together with the optimal deflector shape design, optimal NPR unit cell configuration, and optimal NPR material distribution to significantly improve the protection while minimizing the C.G. height of the vehicle and the weight of the deflector. Structures fabricated using this new concept (combining material configuration, shape and adaptivity) can react to the explosion and reconfigure themselves under the blast force to provide maximum blast protection.

The presented research work consists of two basic approaches to deflector design: optimal deflector shape design and optimal NPR material configuration and distribution in the innovative deflector. In addition, effective material properties of the NPR material with respect to the design variables of the NPR material are first investigated to highlight the unique features of the NPR material and fundamental mechanisms for improved blast protection with reduced weight. The proof-of-concept studies include virtual prototyping using a commercial code of nonlinear dynamic analysis, physical testing through mechanical, drop tower, and blast tube tests. A novel functionally-graded NPR deflector concept is then presented in this paper and the R&D work on the optimal deflector shape design is further highlighted.

THREE-DIMENSIONAL NPR STRUCTURES

A two-dimensional (2D) NPR material was presented in [7], whose configuration was originally suggested by Larsen, et al. in 1997 [9]. Figure 2 illustrates a generalized configuration of such two-dimensional NPR material. Three design variables are associated with the configuration of a unit cell, where, design variable θ_1 denotes angle of the V shape formed by the two adjacent stuffer members, θ_2 denotes the V angle of the two adjacent tensor members, and h is the distance between two vertexes, C and D, of the V shapes in the unit cell. Assuming a symmetrical configuration about the vertical centerline passing through CD, these three design variables uniquely define the geometry of the unit cell and thus the basic configuration of the NPR material. Other design variables associated with the NPR material are cross-section shape, its variation along the length, and material properties of the stuffer members, and

those for the tensor members, which will also have significant effects on the effective material properties of the NPR material. One major feature of this material design is that the tensors and stuffers can be made of different materials that can best suit the functional requirements of the tensors and stuffers, respectively, which leads to a function-oriented design for various applications.

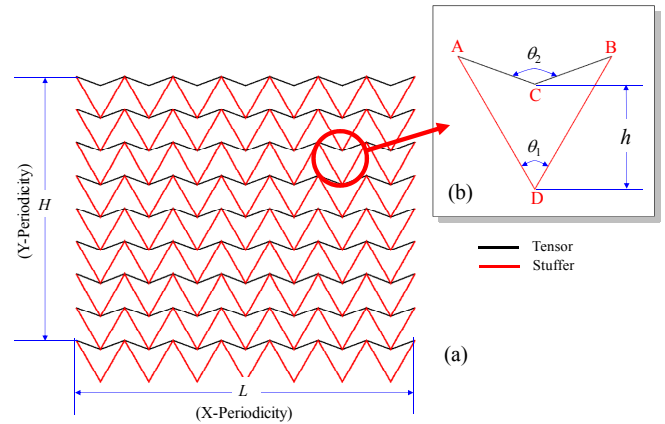


Figure 2: Design variables of the 2D NPR material.

Figure 3 shows two example designs under the assumption of linear constitutive material response but with the consideration of nonlinear geometric effects [7]. Figure 3a illustrates a NPR material design with $\theta_1 = 60^\circ$ and $\theta_2 = 120^\circ$, while Figure 3b illustrates another design with $\theta_1 = 30^\circ$ and $\theta_2 = 60^\circ$. Figure 3 also illustrates the predicted deformation shapes and effective material properties of the two designs, in which, ν denotes the effective Poisson's ratio of the NPR material, and E is the effective Young's modulus. In Figs. 3a and 3b, dashed lines represent the undeformed shape, and solid lines represent the deformed shape. Comparing Figs. 3a and 3b, it is seen that the deformation shapes of the two designs are very different under the same loading condition (a evenly distributed pressures $p = 200$ MPa on the top of the sampling material). The effective Poisson's ratio changed from $\nu = -0.96$ to $\nu = -7.4$ from design (a) to design (b), while the effective Young's modulus changed from $E = 1.4$ GPa to $E = 2.7$ GPa. This suggests that NPR material can be tailored for desired material properties to suit different application needs, especially for the function-oriented material design [10].

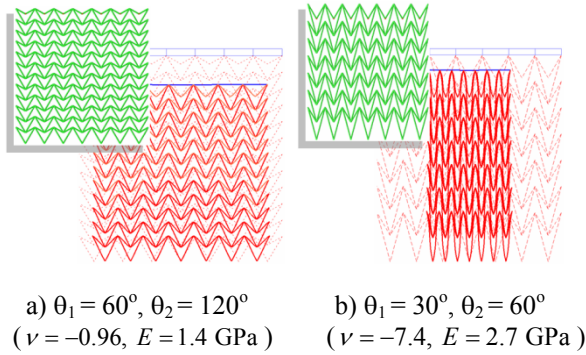


Figure 3: Two example NPR material samples.

Figure 4 illustrates another investigation on the NPR material, showing how the effective material properties, namely, Young's modulus and Poisson's ratio, vary with respect to the design variables θ_1 and θ_2 in a given design domain $\Omega = \{10^\circ \leq \theta_1 \leq 160^\circ, 20^\circ \leq \theta_2 \leq 170^\circ, \text{ and } \theta_1 < \theta_2\}$. As shown in Fig. 4, the effective Young's modulus can vary from 60.3 MPa (at $\theta_1 = 160^\circ$ and $\theta_2 = 170^\circ$) to 6.1 GPa (at $\theta_1 = 10^\circ$ and $\theta_2 = 170^\circ$), and any value in between can be obtained by changing the two design variables. Also, as shown in Fig. 4, the effective Poisson's ratio can be as low as -59.5 (when $\theta_1 = 10^\circ$ and $\theta_2 = 20^\circ$), and any negative value larger than -59.5 can be obtained by changing the two design variables. Note that with a negative θ_2 , effective Poisson's ratio will become positive.

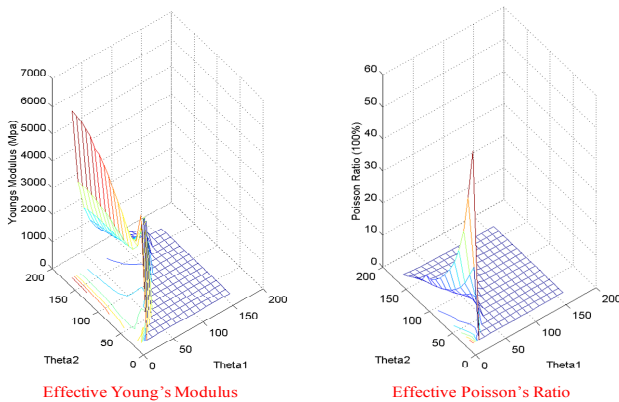


Figure 4: Effective material properties w.r.t. design variables θ_1 and θ_2

The two-dimensional NPR material shown in Fig. 2 has been extended to a three-dimensional (3D) version of NPR materials with a number of variations depending on the arrangement and configuration of the NPR cells. Figure 5

illustrates an example 3D NPR material, while Fig. 6 shows a prototype of such material made of stainless steel, fabricated at MKP Inc. using an innovative manufacturing process. The 3D NPR material has five design variables as shown in Fig. 5, where θ_{1x} and θ_{1y} are angular design variables associated with the stuffer members, θ_{2x} and θ_{2y} are angular design variables associated with the tensor members, and h is the distance between the two vertexes, E and F. Note that similar to the 2D NPR material, other design variables include: cross section geometries, variation of the cross section along the length, material properties of the stuffer and tensor members.

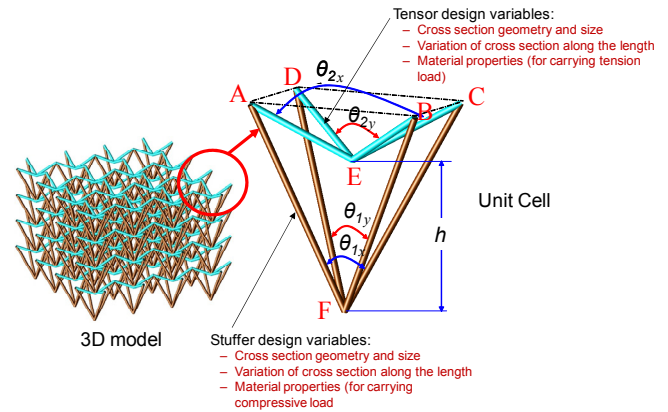


Figure 5: Design variables of the 3D NPR material.

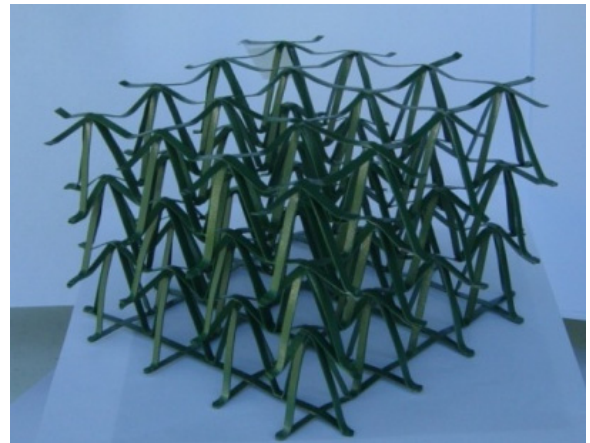


Figure 6: Example prototype of the 3D NPR material (made of stainless steel at MKP).

As a basic study, the unit cell in Fig. 5 is assumed to have axial symmetry about the centerline passing through the vertexes E and F; then $\theta_{1x} = \theta_{1y}$, and $\theta_{2x} = \theta_{2y}$. Figures 7-8

Functionally-Graded NPR (Negative Poisson's Ratio) Material for a Blast-Protective Deflector

illustrate how the effective Young's modulus and Poisson's ratio vary with respect to the design variables $\theta_1 = \theta_{1x} = \theta_{1y}$ and $\theta_2 = \theta_{2x} = \theta_{2y}$ in a given design $\Omega = \{30^\circ \leq \theta_1 \leq 150^\circ, 40^\circ \leq \theta_2 \leq 160^\circ, \text{ and } \theta_1 < \theta_2\}$ with a given set of the parameters for the cross-section areas and material properties of the stuffer and tensor members. As shown in Fig. 7, the effective Young's modulus can vary from 23.2 MPa (at $\theta_1 = 150^\circ$ and $\theta_2 = 160^\circ$) to 6.1 GPa (at $\theta_1 = 50^\circ$ and $\theta_2 = 60^\circ$), and any value in between can be obtained by changing these two design variables. Also, as shown in Fig. 8, the effective Poisson's ratio can be as low as -77 (at $\theta_1 = 40^\circ$ and $\theta_2 = 50^\circ$), and any negative value larger than -77 can be obtained by changing these two design variables. Note that similar to the 2D NPR material, with a negative θ_2 , effective Poisson's ratio will become positive.

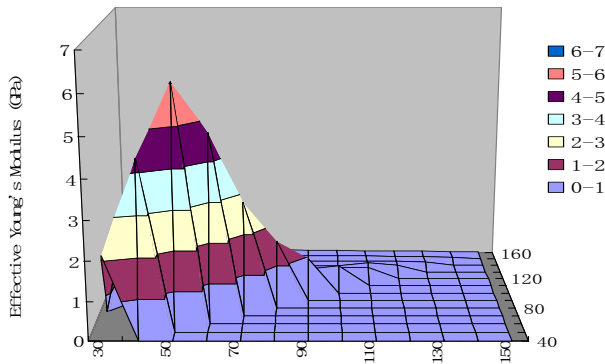


Figure 7: Effective Young's Modulus with respect to design variables θ_1 and θ_2 .

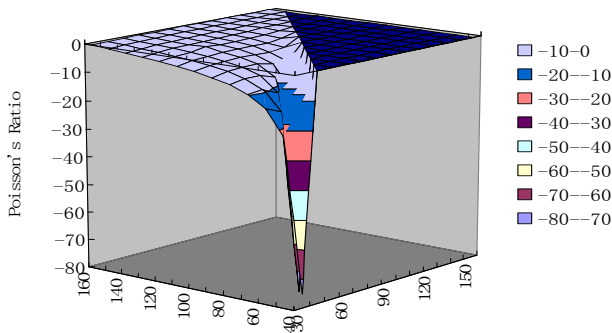


Figure 8: Effective Poisson's ratio with respect to design variables θ_1 and θ_2 .

MAJOR FEATURES OF THE NPR MATERIAL

Figure 9 illustrates three major features of the 3D NPR material: a) Material concentration, b) Bulging effect, and c) Impact force mitigation. Figure 9a illustrates the material concentration effect with an example virtual prototype, where localized pressure is applied to a NPR material. The original material configuration is shown in dashed lines, and solid lines illustrate the deformed NPR material obtained from the simulation. As shown in Fig. 9a, the surrounding material is concentrated into the local area due to the negative Poisson's ratio effect as the force is applied. Therefore the material becomes stiffer and stronger in the local area. This suggests that more material can be gathered together to resist the external load, which can be extended with more advanced design considerations, so that advanced structures can be developed for specific military and commercial applications.

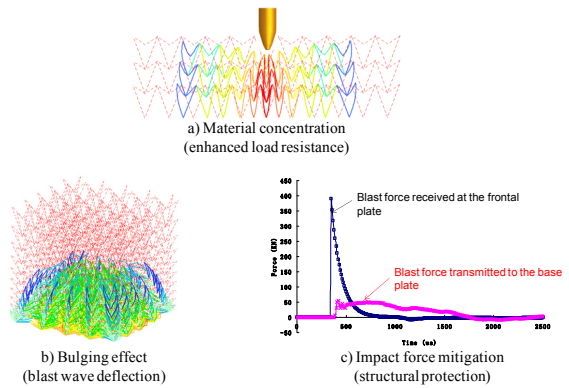


Figure 9: Major features of the 3D NPR material.

Another useful feature of the NPR material is the *Bulging* effect shown in Fig. 9b, which may be used to build a reactively adaptive deflector. A representative reactive mechanism has been developed by incorporating negative Poisson's ratio material in the design. A flat 2D NPR structure is shown in Fig. 10a. Both tensors and stuffers are made of steel, and the top and bottom plates are made of aluminum. The structure has a length of 1,010 mm and a thickness of 495 mm. The unit cell frequencies in the x and y directions are 16 and 12, respectively. Cell unit height is 40 mm and the angles θ_1 and θ_2 are 60° and 130° , respectively. Thickness and width of tensile materials are 2.0 mm and 5.0 mm, respectively, while the width and thickness of stuffer materials are 3.0 mm and 5.0 mm, respectively. As shown in Fig. 10a, a 3 kg TNT explosive charge was placed 400 mm below the bottom plate of the NPR structure.

The calculated blast loading history (the total blast force received at the front surface) on the NPR sample is shown in Fig. 10b, and the structure deformation at three time instants are depicted in Fig. 11. It is seen that the original flat structure deforms to a bulging arc shape during the blast wave attack. This will help to deflect more blast force and reduce the blast load on the structure.

Figure 9c shows another major feature of the NPR material, namely impact force mitigation, as discussed in the following.

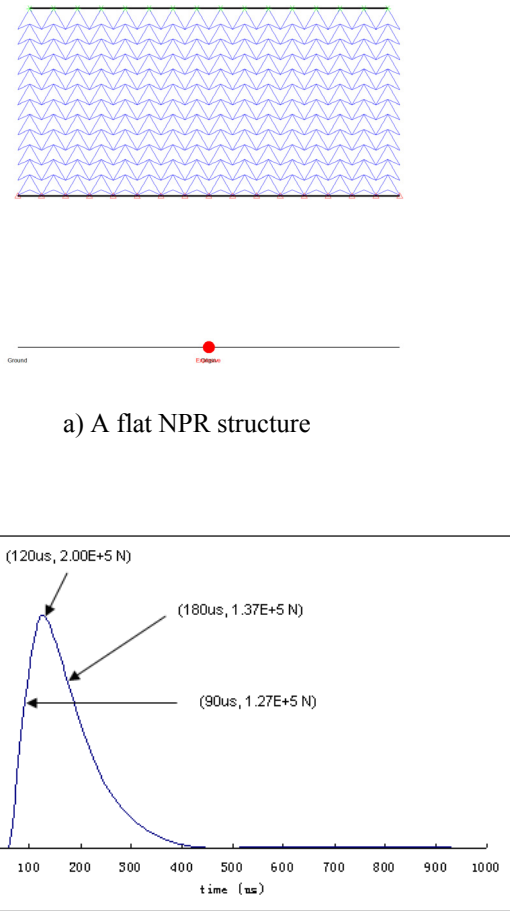


Figure 10: A flat NPR structure and its blast loading history

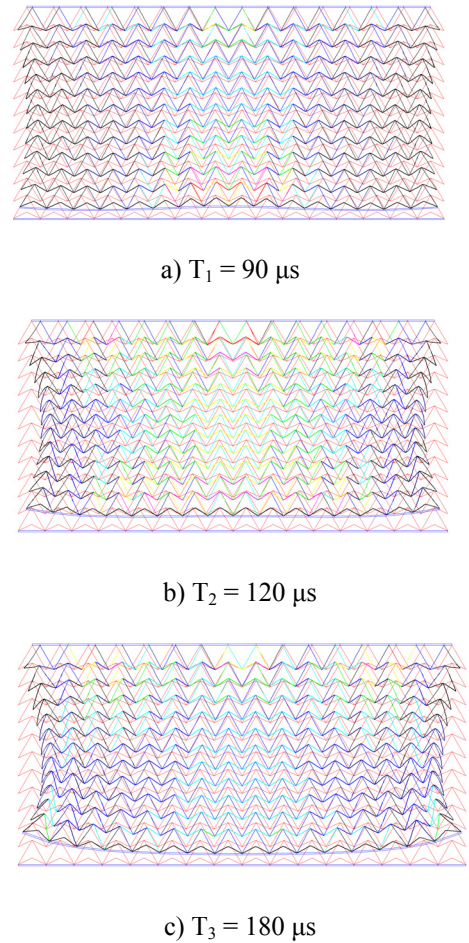


Figure 11: Deformation of a flat deflector at different time moments during a blast attack

VIRTUAL PROTOTYPING WITH COMMERCIAL CODE

To validate major features of the NPR material, a commercial code is used to conduct a virtual prototyping. A flat 3D NPR-based structure is used to demonstrate how this NPR material responds to a blast load. The model is described in Fig. 12 with the following features: 140 mm x 140 mm x 96.8 mm in dimensions; the top and bottom plates are made of aluminum, while the material for the NPR structure is steel; the thickness and width of the NPR tensile members are 2.0 mm and 5.0 mm, respectively; the thickness and width of the stuffer members are 3.0 mm and 5.0 mm; the thickness of the top and bottom plates is 4 mm. Periodicity of the NPR cell is 4 x 4 x 4. For each unit cell, design angles θ_1 and θ_2 (as shown in Fig. 2) are 60° and 130° , respectively. An explosive with 5 kg TNT mass is

placed above the top plate of the NPR structure at different values of standoff distance discussed below.

Figure 13 shows the resultant maximum structure deformations obtained from blast simulation with three different standoff distances of the explosive, 100 cm, 75 cm, and 50 cm, respectively. It is seen that a bulging surface is formed under the blast pressure and the closer the explosive, the larger the resultant bulging of the structure, which results in greater deflection of the blast shock wave.

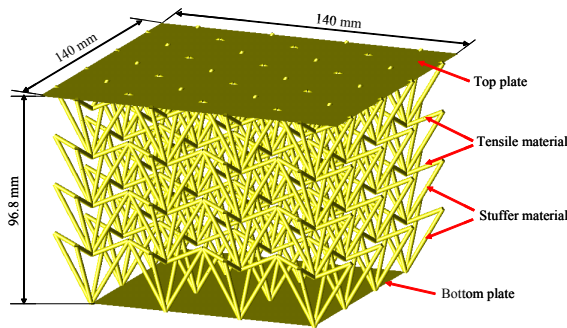


Figure 12: Virtual model of a 3D NPR based structure.

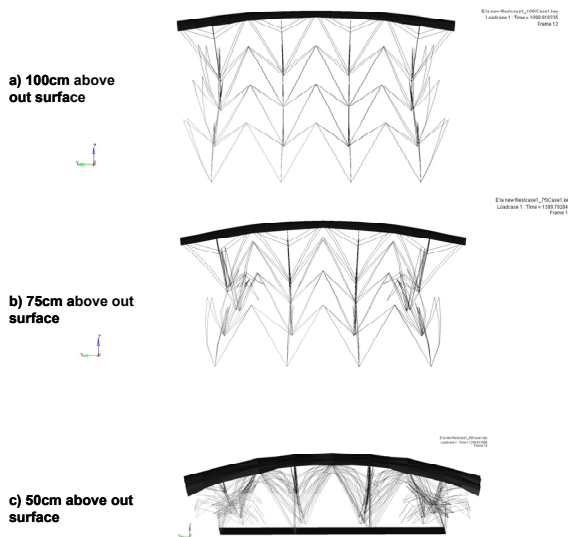


Figure 13: Maximum structure deformations for three different explosive distances.

Figure 14 compares the blast force time history acting on the top plate and the force transferred to the foundation of the structure through the NPR structure for the case shown in Fig. 12 with an explosion distance of 100 cm from the top plate. It is seen that the NPR material largely mitigates the detonation loading and transfers only a small portion of the peak force to the base of the structure. In this particular case, the total peak force transferred to the base structure is only one fourth of the blast loading. Therefore, about 75% of the blast force was deflected or absorbed by the NPR structure.

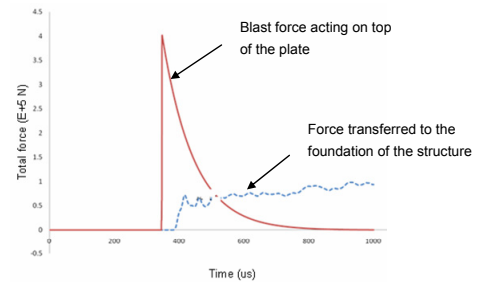


Figure 14: Blast loading versus reaction force on the vehicle.

The blast blocking capability discussed above can be increased by filling the NPR structure with energy absorbing materials. During a shockwave attack, the filling materials within the NPR structures could have permanent deformations, and in doing so a large amount of blast energy could be absorbed. As a result, the blast energy transferred to the vehicle will be further decreased. Energy absorbing materials could be foam, polymer, jelly, or other available materials.

The above simple examples have shown how a NPR-based structure improves its protection by redistributing its materials and adapting its shape in a blast event without utilizing extra energy supply. Using the new design possibilities for three-dimensional designs, more advanced blast-protective structures can be designed and tailored to a wide range of applications.

PHYSICAL TESTS

In order to prove the concept of the novel reactive NPR material, prototypes and test coupons were manufactured, and underwent extensive testing including in-house quasi-static tests, drop tower tests, blast tube tests, and field blast tests to evaluate various NPR-based structure designs, especially their potential to deflect blast forces and absorb blast energy.

Prototype Development

A special stamping machine, metal forming machine, and multi-point welding machine were designed and fabricated by MKP. MKP has fabricated a large number of NPR-based structures; examples are shown in Fig. 15.

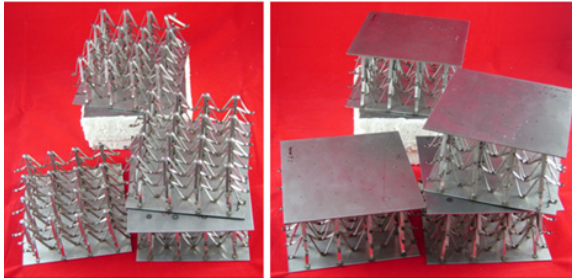
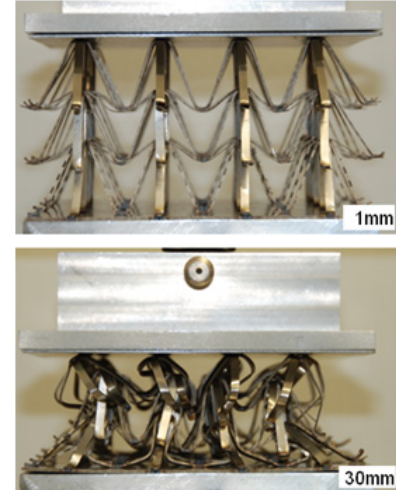


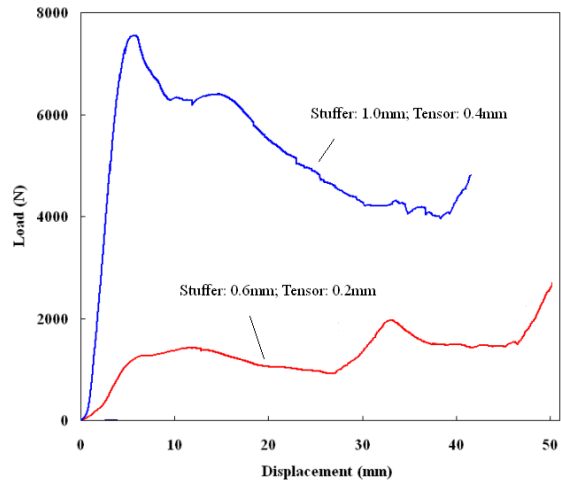
Figure 15: NPR-based structures fabricated.

Mechanical Tests

Two quasi-static compression tests on the NPR materials were performed in MKP’s lab. Stuffer thickness and tensor thickness are 1.0 mm and 0.4 mm respectively for the first sample, and 0.6 mm and 0.2 mm for the second sample. The experimental setup is shown in Fig. 16a. Steel plates are placed at top and bottom of NPR material for applying uniform loading. The experiment was performed under displacement control with cross-head displacement rate of 1 mm/min. Images for Test 1 are shown in Fig. 16a. The material clearly shows a negative Poisson ratio response under the compressive loading. The reaction load as a function of cross-head displacement is shown in Fig. 16b. Comparison of above two test results shows that thickness of stuffer and tensor has significant effect on the mechanical properties of the NPR samples. NPR material with stronger stuffer and tensor demonstrates much higher stiffness and strength.



a) Experimental setup and deformation of the NPR sample under a quasi-static compressive load



b) Load-displacement curves of NPR compressive tests

Figure 16: Compression test of a NPR sample.

Drop Tower Test

A drop tower test with drop height of 14 feet was set up at MKP, using a drop weight of 50 kg. Calculations based on the data provided by [11-14] indicate that the incident impulse provided by the drop weight on a 6”X6” specimen is within the similar range of a standard blast test (6 kg TNT, 0.5 m from the specimen). The load transmitted to the specimen was monitored by means of a load cell placed under the sample. A camera was used to capture deformation images. Four samples with same overall dimensions were tested to study the major features of the NPR structures. The four samples tested are:

Functionally-Graded NPR (Negative Poisson's Ratio) Material for a Blast-Protective Deflector

UNCLASSIFIED: Dist A. Approved for public release

- TST61: Without NPR. (Drop weight impact right on the load cell.)
- TST62: NPR filled with foam: Stuffer thickness is functionally-graded with different stuffer thicknesses in different layers, which are 1 mm, 1.2 mm, and 1.8 mm, for layers 1, 2, and 3, respectively;
- TST63: NPR without foam: Stuffer thickness is 1 mm;
- TST64: NPR filled with foam: Stuffer thickness is 1 mm.

Images from the drop tower test (TST64) are shown in Fig. 17. Figure 18 shows the compressive strain measured at the load cell during the testing process. Impact load proportional to the compressive strain was calculated and is plotted in Fig. 19. Tests without NPR materials demonstrate a much larger impact load than tests with NPR. Deformations of the NPR samples are also shown in Fig. 19. It is seen that NPR samples tested significantly reduce the impact load transferred to the load cell (by 50%-90%). Test results also show that the polymer foam can reduce 36% of the transferred impact load with a small increase of the sample weight, while reducing by 70% the deformation of the NPR.

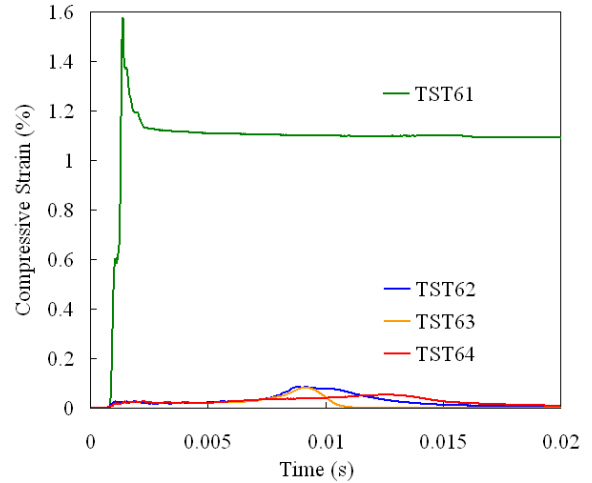


Figure 18: Drop tower tests.

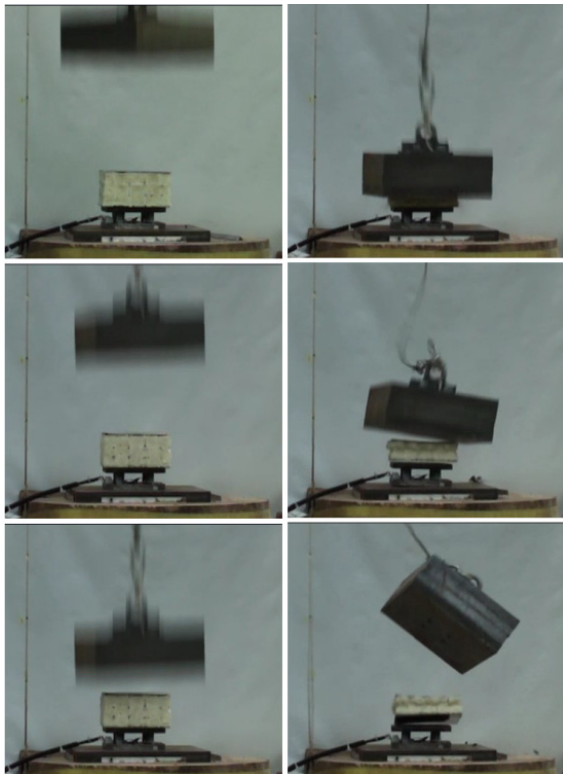


Figure 17: Snapshots of the drop tower test.

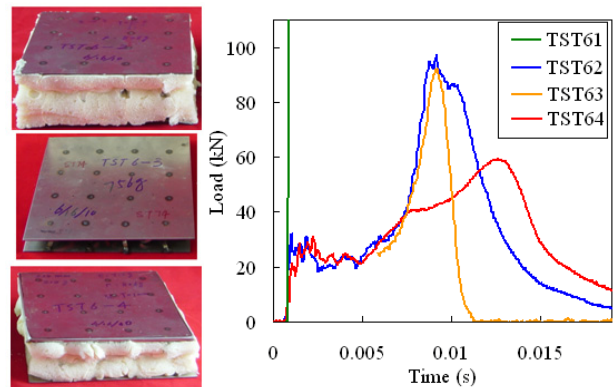
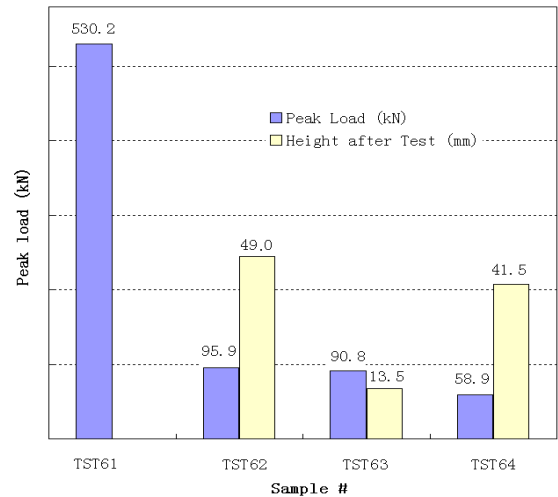


Figure 19: Peak loads and deformation for drop tower tests on NPR materials.

Functionally-Graded NPR (Negative Poisson's Ratio) Material for a Blast-Protective Deflector

UNCLASSIFIED: Dist A. Approved for public release

Shock Tube Tests

Shock tube tests were conducted at Composite Structures Laboratory (directed by Dr. Anthony Waas) at the University of Michigan. The testing setup is shown in Fig. 20. Specimens are placed inside a cylinder fixture, which is connected to the shock tube. As the shock wave travels down the shock tube, pressure transducers sense the passing shock wave and trigger the oscilloscope. Shown in Fig. 21a are the internal structures of a NPR-based sample and a square honeycomb. Two samples are fabricated with the same mass density and tested at the identical blast condition. The square honeycomb core structures are fabricated based on [15]. Figure 21b shows the samples after the blast tube tests. It is seen that the tested NPR sample having a convex shape, while the square honeycomb sample a concave shape. This clearly demonstrates the advantages of NPR-based structures in defeating blast loading if it is used for a blast protective deflector.

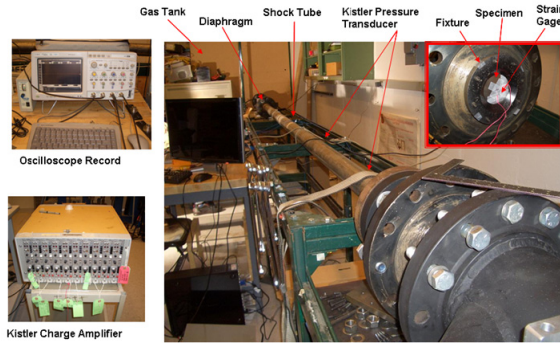
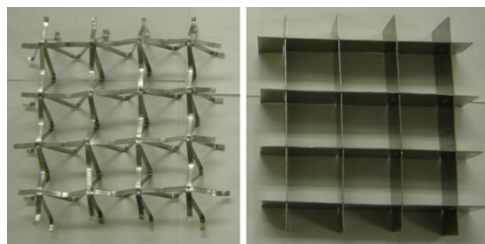


Figure 20: Shock tube at U of M Composite Structures Laboratory.



a) NPR & honeycomb core structures to be tested.



b) Deformed samples after blast tube testing

Figure 21: Comparison of NPR-based structure with a standard square honeycomb structure.

FUNCTIONALLY-GRADED NPR DEFLECTOR CONCEPT

The NPR material concept is further extended to a functionally-graded NPR structure concept. In this section, we focus on the design of special NPR deflectors that feature non-uniform stiffness, in such a way as to more easily deform to a predefined optimal shape upon blast attack and thus enhance the blast wave deflection capability.

Figure 22 shows a functionally-graded material concept for a reactive deflector. In this concept, stronger material is distributed near the center of the deflector while weaker materials are near the edges. Prior to the arrival of blast wave, the deflector has normal (flat) configuration. Under a blast load, the deflector will deform as shown in Fig. 22b due to the designated strong/weak material distribution. Consequently, the deflector will react to the blast energy by changing its shape so that the blast load delivered to vehicle body is minimized.

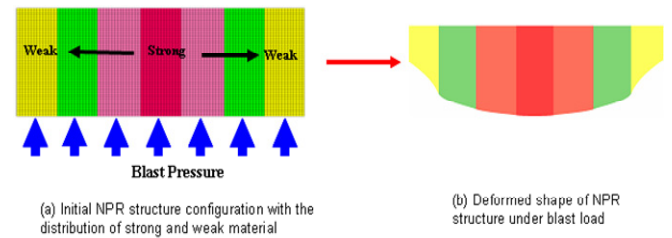


Figure 22: Comparison of total vertical blast impulses versus TNT position for different deflector designs.

The concept shown in Fig. 22 can be realized by imbedding NPR material in a functionally-graded way as shown in Fig. 23. The structure is specially designed to have non-uniform stiffness distribution by controlling the design angles θ_1 and θ_2 . Figure 23 illustrates how the NPR structure changes with respect to θ_1 , while angle θ_2 is kept constant. As the result, towards the center the structure becomes increasingly stiffer.

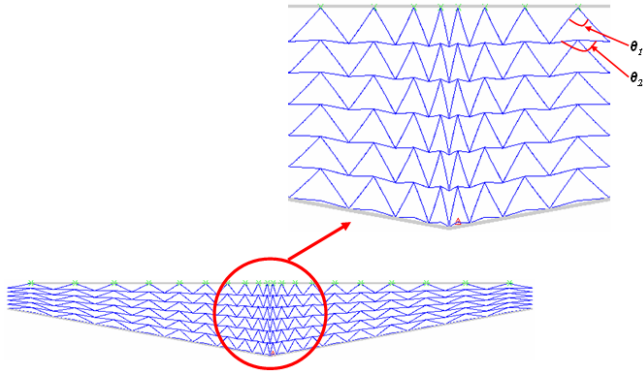


Figure 23: A flat NPR structure and its blast loading history

A typical V-shape deflector based on the above non-uniform stiffness concept has been modeled as shown in Fig. 24. This structure is made of steel. The cross section of the tensile material is 2 mm X 5 mm, and the stuffer material cross section is 3 mm X 5 mm. The top and bottom plates have a thickness of 4 mm. A 5 kg TNT explosive charge was placed 500 mm below the bottom of the NPR structure. It can be seen that along the lateral direction, the material stiffness increases and reaches maxima at the center.

Under explosive loading, the deformation of the V-shape deflector in Fig. 25 was calculated based on a quasi-static analysis. Figures 25a-c show the blast pressure on the deflector (top figures) and structure deformation (bottom figures). As shown in Fig. 25, the deflector is deformed to a sharper angle under blast load during the interaction with the blast wave, which results in better deflection of the blast shock wave. Therefore, less blast load will be transferred to the vehicle main structure. This indicates that the effectiveness of the deflector can be significantly improved by simply inducing the shape adaptivity that is resultant from the (NRP) reactive mechanism we designed.

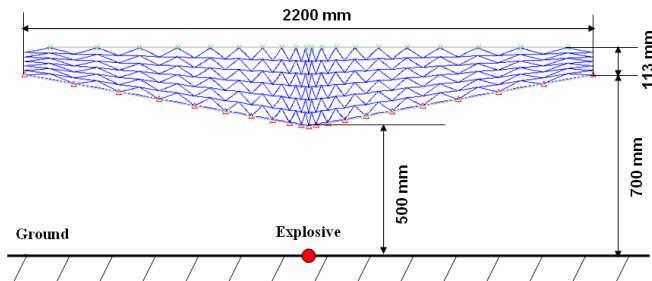
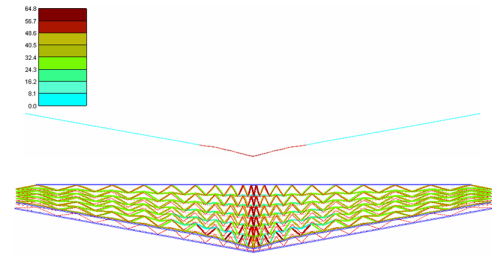
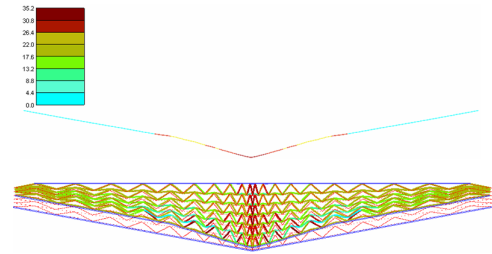


Figure 24: Simulation model of the FG-NPR deflector

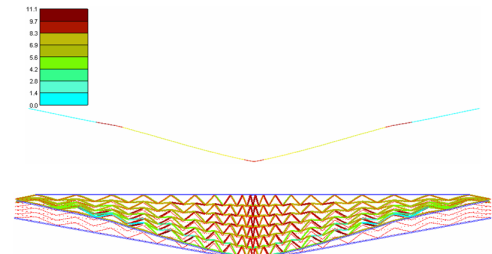
Functionally-Graded NPR (Negative Poisson's Ratio) Material for a Blast-Protective Deflector



a) T=150 μ s



b) T=210 μ s



c) T=330 μ s

Figure 25: Deformation history of the deflector under a quasi-static blast load.

DEFLECTOR SHAPE OPTIMIZATION

It has been found that the shape of the deflector has a critical influence on blast protection. Deflector shape optimization was performed with deflector shapes represented as B-Spline surfaces. The total blast impulse exerted on a deflector was selected as the objective function, and maximum instant blast force was used as design constraint. For a given design domain, deflector shape is determined by varying control points A, A', and B as shown in Fig. 26 for varied explosion position along the lateral direction. From the optimization, a W-shape geometry was seen to outperform the all other possible shapes that can be described by the B-Spline, which include traditional flat, concave-V, and V-shape designs.

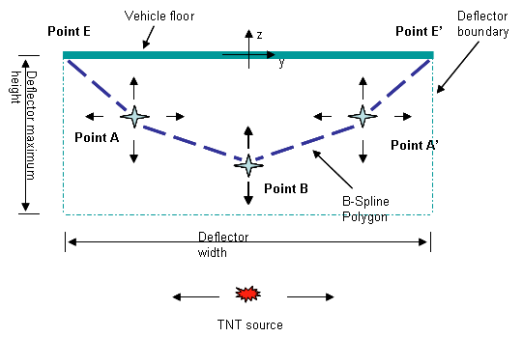


Figure 26: Deflector geometry design boundaries.

Virtual prototyping via commercial software confirms that the W-shape deflector not only provides better protection in terms of the impact load, but also minimizes the turn-over possibility upon the offset TNT detonation.

Figure 27 illustrates a finite element model developed for a W-shape deflector with a dummy model, which is used for the virtual prototyping. Figure 28 shows the comparison of total vertical blast impulses of three deflector designs namely, flat design, V-shape design and optimal W-shape design, versus TNT lateral position in a given design circumstance. It is observed that in terms of total blast impulse, W-shaped deflector gives even better results when TNT is closer to the vehicle center.

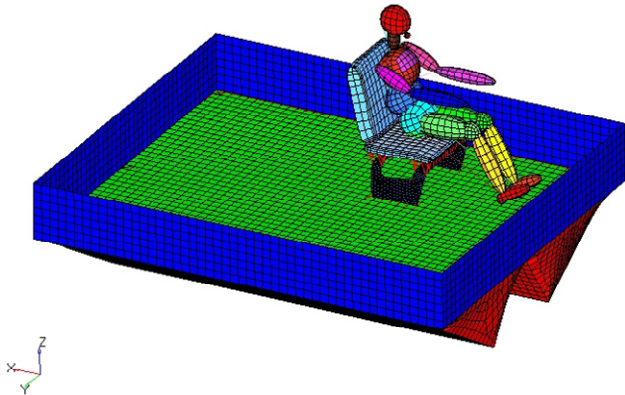


Figure 27: Finite element model of a W-shape deflector with dummy

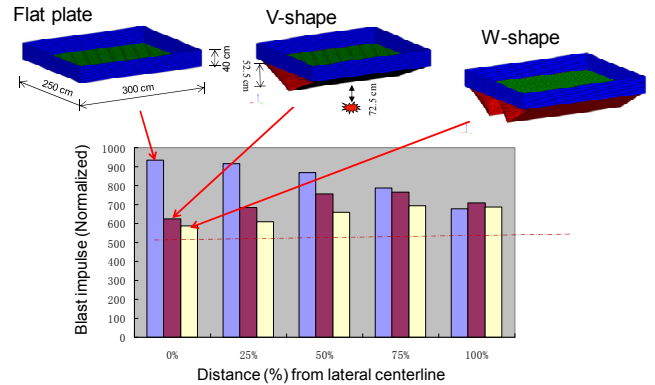


Figure 28: Comparison of total vertical blast impulses versus TNT position for different deflector designs.

Optimal deflector shape design and optimal NPR material distribution is being integrated into the final design of the blast protective deflector to further improve the deflector's blast defeating performance.

CONCLUSIONS

A functionally-graded NPR (Negative Poisson's Ratio) material concept is being developed for a blast-protective deflector, which can concentrate material into the areas most needed and adapt its shape utilizing the blast energy to improve blast mitigation and crew protection. This effort is also combined together with the optimal deflector shape design, optimal NPR unit cell design and optimal NPR material distribution to further improve the protection while minimizing the C.G. height of the vehicle and the weight of the deflector.

ACKNOWLEDGEMENTS

Blast-protective deflector research is supported by the U.S. Army TARDEC under Contract No. W56HZV-09-C-0037 through MKP Structural Design Associates, Inc. Shock tube tests were conducted at Composite Structures Laboratory (directed by Dr. Anthony Waas) in the Department of Aerospace Engineering at the University of Michigan.

REFERENCES

1. R. Lakes, "Foam Structures with Negative Poisson's Ratio", Science, Vol. 235, No. 4792, pp1038-1040 (1987).
2. Lakes R. S. Advances in negative Poisson's ratio materials, Advanced Materials, 1993.-Vol.5.- P.293-296.
3. K. E. Evans and A. Alderson, "Auxetic Materials: Functional Materials and Structures from Lateral

- Thinking”, *Advanced Materials*, Vol. 12, No. 9, pp617-628 (2000).
4. G. E. Stavroulakis, “Auxetic behavior: appearance and engineering applications”, *Phys. Stat. Sol. (b)*, Vol. 202, No. 3, pp710-720 (2005).
 5. Alderson, K. L., Alderson, A., Smart, G., Simkins, V. R., and Davies, P. J., “Auxetic polypropylene fibres, Part I. Manufacturing and characterization”, *Plast. Rubbers Compos*, 31(8), pp344-349 (2002).
 6. Alderson and K. L. Alderson, “Auxetic Materials”, *Proc. IMechE Vol. 221, Part G: J. Aerospace Engineering*, pp565-575 (2007).
 7. Liu, Y., Ma, Z.-D., “Nonlinear analysis and design investigation of a negative Poisson’s ratio material”, *Proceedings of the ASME International Mechanical Engineering Congress and Exposition, IMECE07*, Nov. 10-16, 2007, Seattle, Washington, USA.
 8. Ma, Z.-D., “Three-Dimensional Auxetic Structures and Application Thereof,” Patent Application Publication, Pub. No.: US 2010/0119792 A1, May 13, 2010.
 9. Larsen, U. D., Signund, O., and Bouwsta, S., “Design and fabrication of compliant micromechanisms and structures with negative Poisson’s ratio”, *Journal of Microelectromechanical Systems*, Vol. 6, pp99-106 (1997).
 10. Ma, Z.-D., Wang, H., Kikuchi, N., Pierre, C. and Raju, B., “Function-Oriented Material Design for Next Generation Ground Vehicles”, 2003 ASME International Mechanical Engineering Congress & Exposition, November 15-1, 2003, Washington, DC.
 11. Structures to resist the effects of accidental explosions, Departments of the Army, the navy, and the air force, 1990
 12. A manual for the prediction of blast and fragment loadings on structures, Unites states department of energy Albuquerque operations office, 1992
 13. W. E. Baker, Blast Pressure Effects: An Overview Wilfred Baker, In *Design Considerations for Toxic Chemical and Explosives Facilities*; Scott, R., et al..
 14. Kingery, C. N., and Bulmash, G., *Airblast Parameters from TNT Spherical Air Burst and Hemispherical Surface Burst*”. Ballistic Research Laboratory Technical Report ARBRL-TR-02555, Aberdeen Proving Ground, MD., 1984.
 15. Kumar P. Dharmasena, Haydn N.G. Wadley, Zhenyu Xue and John W. Hutchinson, Mechanical response of metallic honeycomb sandwich panel structures to high-intensity dynamic loading, *International Journal of Impact Engineering*. Vol. 35, Issue 9, September 2008, Pages 1063-1074.